J Mater Sci (2009) 44:300–305
DOI 10.1007/s10853-008-3066-3

Microstructure and mechanical properties of CrAlN coatings deposited by modified ion beam enhanced magnetron sputtering on AISI H13 steel

Chunyan Yu · Shebin Wang · Linhai Tian · Tianbao Li · Bingshe Xu

Received: 22 October 2007 / Accepted: 15 October 2008 / Published online: 10 November 2008

Abstract CrAlN coatings were deposited on silicon and AISI H13 steel substrates using a modified ion beam enhanced magnetron sputtering system. At the modified ion beam bombardment, the effects of bias voltage and Al/(Cr + Al) ratio on microstructure and mechanical properties of the coatings were studied. The X-ray diffraction data showed that all CrAlN coatings were crystallized in the cubic NaCl B1 structure, showing the (111), (200), and (220) preferential orientation. It is noted that the (111) diffraction peak intensity decreased and the peaks broadened as the bias voltage increased at the same ratio of Al/Cr targets power, which is attributed to the variation in the grain size and microstrain. The microstructure observation of the coatings by field emission scanning electron microscopy cross-section morphology shows that the columnar grain became more compact and dense with increasing substrate bias voltage and Al concentration. At a substrate bias voltage of −120 V and a Al/(Cr + Al) ratio of 40%, the coating had the highest hardness (33.8 GPa) and excellent adhesion to the substrate.

C. Yu · S. Wang · T. Li · B. Xu (✉)
College of Materials Science and Engineering, Taiyuan University of Technology, Yingze Street 79, Taiyuan 030024, China
e-mail: xubs@tyut.edu.cn

S. Wang · T. Li · B. Xu
Key Laboratory of Interface Science and Engineering in Advanced Materials, Taiyuan University of Technology, Ministry of Education, Taiyuan 030024, China

L. Tian
Research Institute of Surface Engineering, Taiyuan University of Technology, Taiyuan 030024, China

Introduction

As a kind of hotworking die steel, AISI H13 steel undergoes wear caused by mechanical action of light alloy injected under a high pressure, corrosive attack of melting alloy, thermal cycling, and high-temperature corrosion (oxidation). Hard coatings can protect the steel surface very efficiently from chemical attack by casting alloys and retard the formation and propagation of thermal cracks [1]. Chromium nitride is a typical transition metal nitride coating with high hardness, good wear resistance and corrosion resistance and is widely used in die casting, metal forming, and tool machining applications to increase productivity and tool life [2, 3]. But the oxidation resistance of CrN is limited up to 600 °C [4]. For hard protective coatings, thermal stability is important as they are exposed to high temperatures during casting process. Chromium aluminum nitride (CrAlN), a ternary nitride, by incorporating Al into transition binary CrN thin coatings has been intensively investigated in recent years [5–18]. Compared with CrN coatings, CrAlN coatings exhibit higher hardness, lower friction coefficient [8, 17], and higher thermal stability with no compositional and structural changes after annealing at 800 °C [8] and at 900 °C [19]. Therefore, CrAlN coating is a good candidate as an alternative to conventional CrN coatings especially for high-temperature oxidation-resistance applications.

CrAlN coatings have been successfully produced through different physical vapor deposition (PVD) methods such as DC magnetron sputtering [7, 15, 16], arc ion plating [17], and cathodic arc evaporation [5, 18]. Pulsing the DC magnetrons has also been shown to facilitate ion bombardment and greatly improve film density and film properties [20–24]. Recently, a novel type of gaseous ion source, driven by a dedicated pulsed DC power supply, has

been successfully developed. In this equipment, metal sputtering deposition, reactive ion beam bombardment, and reaction are performed separately. The advantages of the newly modified technique include easy operation, long time stability, good repetition, consistency and growth of high quality film. In this study, a series of CrAlN coatings were deposited on silicon and AISI H13 steel substrates by modified ion beam enhanced magnetron sputtering from Cr and Al elemental targets in an Ar + N_2 mixture atmosphere. At the modified ion beam bombardment, the effects of bias voltage and Al/(Cr + Al) ratio on microstructure and mechanical properties of the coatings were studied.

Experimental

The substrate materials are silicon and AISI H13 steel. Silicon substrates were used for the test of morphology, structure and hardness and AISI H13 substrates were used in performance of coatings composition and adhesion. AISI H13 has a composition of 4.90 wt.% Cr, 1.06 wt.% V, 0.34 wt.% Mn, 1.25 wt.% Mo, 0.39 wt.% C and Fe in balance. The hardness of AISI H13 steel is about 50 HRC after quenching and tempering. The dimensions of AISI H13 sample were 2 × 1 × 0.5 cm, and all the samples were ground and polished to an average surface roughness less than 0.05 μm and then cleaned with acetone in an ultrasonic container for 15 min. Subsequently, they were rinsed in deionized water, dried and stored in a desiccator prior to coating operation. CrAlN coatings were deposited by a modified ion beam enhanced magnetron sputtering system. The detail of the equipment was the same as that described by Dong et al. [25]. Prior to deposition, the targets were sputter cleaned for 3 min. Then the samples were sputter-etched with argon ions (3 Pa, applied bias voltage −500 V) for approximately 10 min to remove surface oxide and pollution. During deposition, the power of gas ion source was 1.2 kW and the substrate temperature was 300 °C. All of the four targets were sputtered using DC power. A transition layer of Cr and Al was deposited to facilitate bonding with the first CrAlN deposited layer. The sputtering power applied onto Al targets was fixed at 3.6 kW. In order to control the atomic ratio of Al/Cr in deposited coatings, the sputtering power applied on Cr targets was selected as 2.4 and 3.6 kW. Correspondingly, the atomic ratio of Al/(Cr + Al) in CrAlN coatings was increased from 0.3 to about 0.4.

The surface and cross-section morphology of coatings were inspected using field emission scanning electron microscopy (FESEM). The crystal structure was analyzed by X-ray diffraction (XRD) using Cu–Ka radiation. The average grain size and microstrain ε of the coatings were determined by the single-line method for analysis of XRD line broadening using a Voigt profile function. A glow discharge optical emission spectrometer (GDOES) was used to estimate the composition depth profiles of the coatings. To determine adhesion strength, scratch tests were conducted. The failure modes of the coatings were examined after scratch test using scanning electron microscope (SEM) to compare with the results of the recorded acoustic emission signal. Microhardness of the coatings was measured on a standard Vickers hardness machine with Knoop indentation using a load of 0.25 N.

Results and discussion

Figures 1 and 2 show the FESEM cross-section and surface morphology of CrAlN coatings at different Al/Cr targets power ratio and bias voltage. All the CrAlN coatings exhibited a columnar structure, as shown in Fig. 1. At the same substrate bias voltage, the coating exhibited a much denser structure with an increase of Al/Cr targets power ratio (Fig. 1a and c, b and d). At the same ratio of Al/Cr targets power, the coatings thickness decreased with an increase of substrate bias (Fig. 1a and b, c and d). This behavior is clearly due to a partial re-sputtering mechanism induced by the ion bombardment during the coating growth. As the negative bias is increased, the highly ionized flux of Cr and Al atoms arrives to the substrate with a higher kinetic energy, and as a result, a higher number of atoms from the growing coating will be re-sputtered [5]. In Fig. 2, it is clearly noticed that big grains embraced small grains.

Figure 3 illustrates the GDOES depth profiles of the CrAlN coatings deposited on AISI H13 substrate at the Al/Cr targets power ratio of 3/2. Although the atomic compositions deduced from the GDOES analysis cannot be considered as absolute values, the compositional results obtained for the different samples indicate that there was a slight increase of the ratio of Al to Cr as the negative bias increased, which is in accord with the results investigated using energy dispersive spectroscopy (EDS) (as shown in Table 1). This can be attributed to the different sputtering yield of Cr and Al in CrAlN compound [5]. In addition, the Cr and Al elemental chemical composition increased from the coating surface to the substrate because the supply of N_2 was increased gradually to insure the gradient changes of composition and structure of coatings. This is useful to improve bonding strength of CrAlN coatings.

XRD patterns of the coatings are shown in Fig. 4. The CrAlN coatings were crystallized in the cubic structure, showing the (111), (200), and (220) preferential orientation, indicating that the crystalline structures of the CrAlN coatings were predominantly cubic as that of CrN. The peaks fall between those for B1 aluminum nitride (Joint

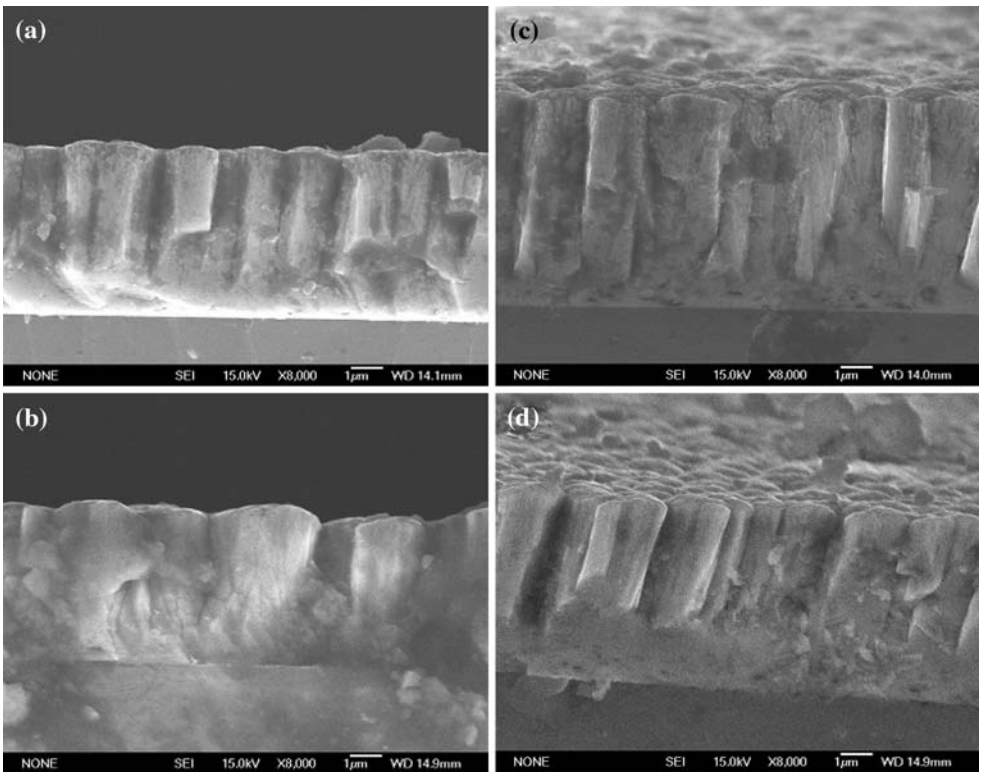

Fig. 1 Cross-section FESEM images of CrAlN coatings under different deposition conditions. **a** Al/Cr targets power ratio = 3/2, bias = 0 V; **b** Al/Cr targets power ratio = 3/2, bias = −120 V; **c** Al/Cr targets power ratio = 1/1, bias = 0 V; **d** Al/Cr targets power ratio = 1/1, bias = −120 V

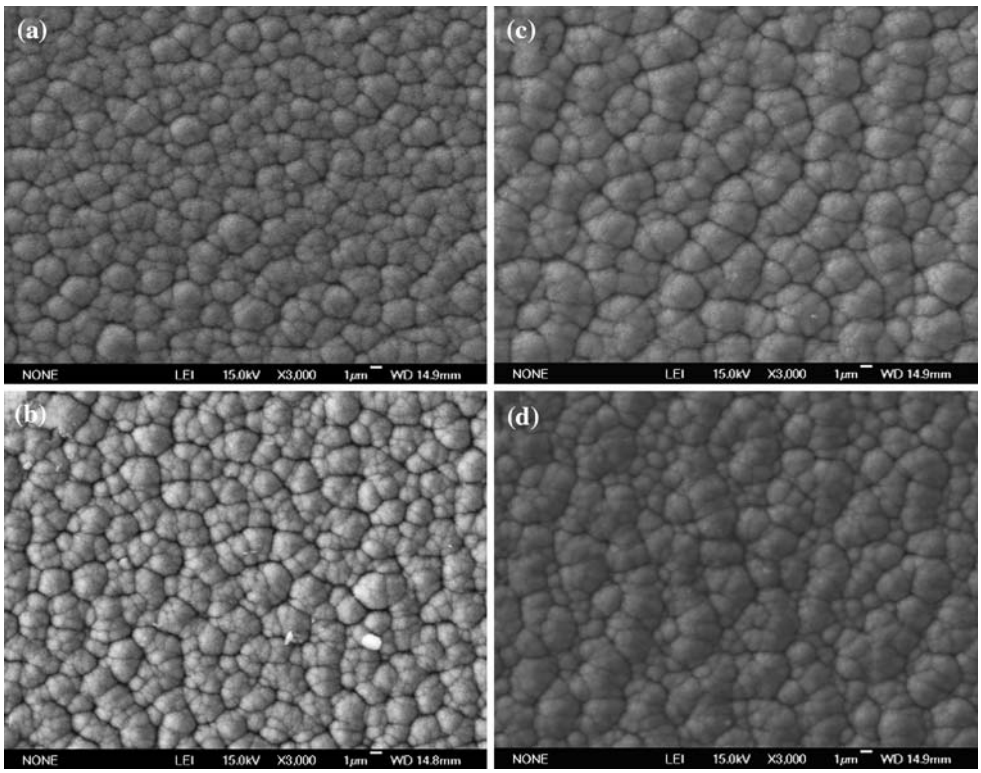

Fig. 2 FESEM surface morphology of CrAlN coatings under different deposition conditions. **a** Al/Cr targets power ratio = 3/2, bias = 0 V; **b** Al/Cr targets power ratio = 3/2, bias = −120 V; **c** Al/Cr targets power ratio = 1/1, bias = 0 V; **d** Al/Cr targets power ratio = 1/1, bias = −120 V

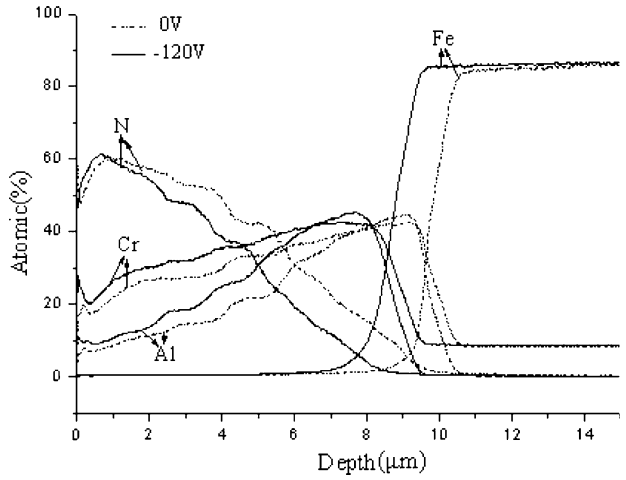

Fig. 3 GDOES depth profiles of CrAlN coatings prepared at the Al/Cr targets power ratio of 3/2

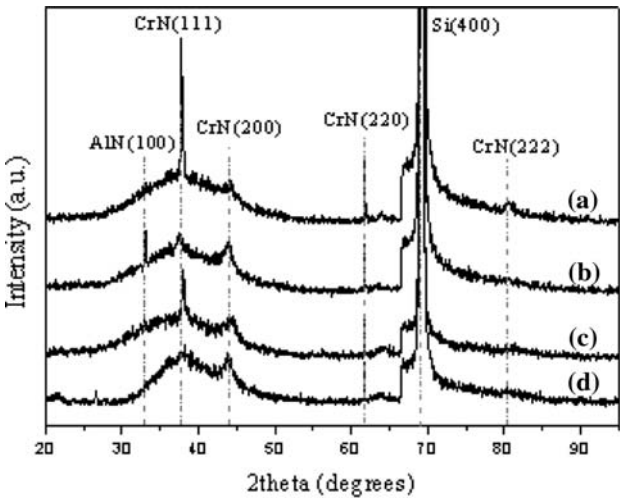

Fig. 4 XRD patterns for different samples. (a) Al/Cr targets power ratio = 3/2, bias = 0 V; (b) Al/Cr targets power ratio = 3/2, bias = −120 V; (c) Al/Cr targets power ratio = 1/1, bias = 0 V; (d) Al/Cr targets power ratio = 1/1, bias = −120 V

Committee Powder Diffraction Standard (JCPDS) Card No. 24-1495) and B1 chromium nitride (JCPDS Card No. 11-0065) [26], which implies complete solubility of chromium, aluminum, and nitrogen in the rock-salt-type lattice. At the same Al/Cr target power ratio, it is also noted that the (111) diffraction peak decreased in intensity and broadened in width as the bias voltage increased, which is attributed to the variation in the grain size and microstrain. With the substitution of Al atoms into the coatings, the lattice parameter of the coating decreases. Using the Voigt profile function to analyze the line profile of the CrN-111 diffraction peak, one can determine the grain size D and microstrain ε that are shown in Table 1. The grain size decreases and the microstrain increases with increasing bias voltage. With increasing substrate bias voltage, the mobility of the adatoms on the substrate surface increased and the shadowing effect of the columnar structure was reduced, resulting in a denser coating with reduced grain size and less columnar. At a substrate bias voltage of −120 V and the Al/Cr targets power ratio of 3/2, AlN diffraction peaks were observed.

Table 1 gives the thickness, grain size, microstrain and microhardness of the coatings grown at different substrate bias voltage and Al concentrations. In several investigations, the hardness of the thin film has also been reported to increase with increasing compressive stress developed during the deposition [27]. In addition, the decrease in lattice parameter and increase in the density of coating microstructure have significant effects on the mechanical properties of CrAlN coatings [28, 29]. It has been reported that incorporation of Al atoms into CrN binary phase can develop amorphous AlN network in grain boundary, which can effectively reduce grain size due to grain boundary effect [30]. Therefore, the increase of hardness of CrAlN coatings with increasing Al content was probably related to high density, the higher residual stress, and lattice constant effect. In this study, the coatings deposited at a bias of 0 V and exhibited low hardness. However, as substrate bias voltage and Al concentration increased, the hardness of CrAlN coatings was dramatically increased to maximum values of 33.8 GPa.

Scratch tests were performed to determine adhesion strength. The acoustic emission (AE) was recorded while a Rockwell C diamond was drawn over the coatings with increasing normal force at a speed of 4 mm/min. The failure mechanisms of the coatings were examined after scratch test by FESEM observation. With an EDS system for compositional analysis, it is possible to determine

Table 1 Elemental compositions and properties of CrAlN coatings deposited under different conditions

The ratio of Al/Cr targets power	Substrate bias voltage (V)	Composition (at.%)				Al/(Cr + Al) (%)	Thickness (μm)	Knoop hardness (GPa)	Microstrain ε	Grain size D (nm)
		Cr	Al	N	Fe					
3/2	0	26.93	15.84	45.84	1.81	37.03	5.07	17.6	0.033566	6.604729
	−120	30.78	20.46	48.15	0.61	40.00	4.85	33.8	0.254416	1.502148
1/1	0	36.14	15.53	48.33	0	30.05	6.38	15.3	0.122812	3.218789
	−120	35.01	14.43	48.56	0	31.60	5.89	20.9	1.23294	2.099842

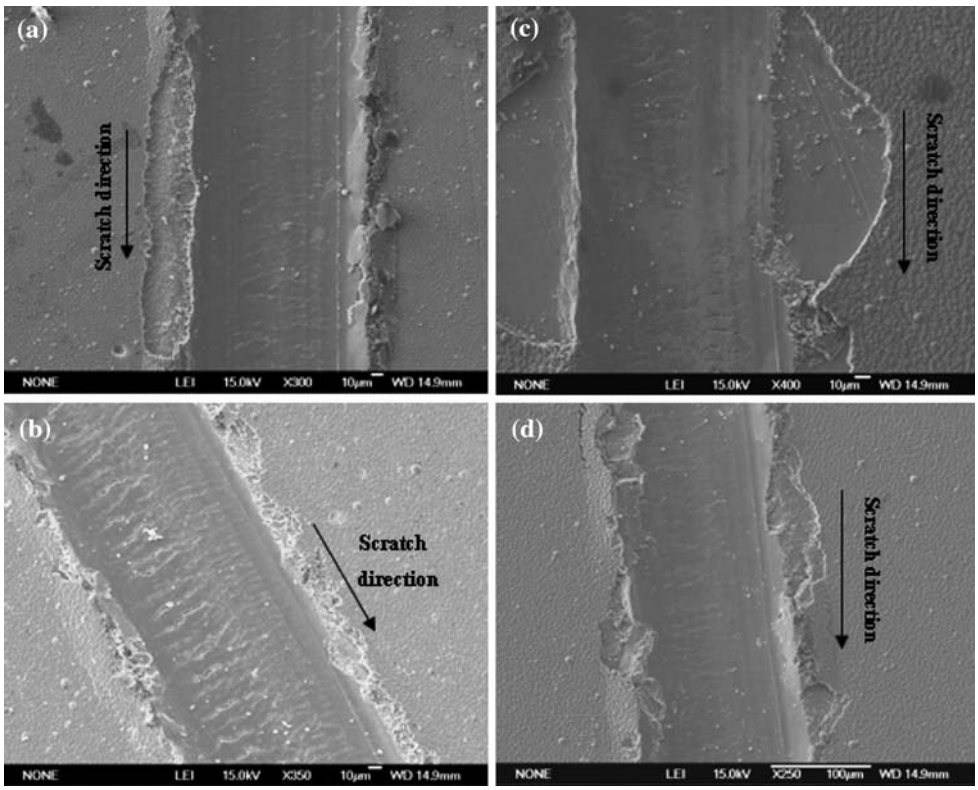

Fig. 5 The tracks of the scratch test near the scope of 50 N force. **a** Al/Cr targets power ratio = 3/2, bias = 0 V; **b** Al/Cr targets power ratio = 3/2, bias = −120 V; **c** Al/Cr targets power ratio = 1/1, bias = 0 V; **d** Al/Cr targets power ratio = 1/1, bias = −120 V

whether the diamond broke through the coating into the substrate or not. In all the samples, the first acoustic emissions signal was detected at about a load of 40 N.

Figure 5 shows the tracks corresponding to the four investigated coating systems after scratch test under the load of about 40–50 N. The diamond flattened the coatings to some extent. In all of the scratch tracks, the chipping increased with increasing indenter load alongside the scratch track. In Fig. 5b and d, the EDS signal received from the track shows chromium, aluminum, nitrogen, and very little iron. At the same substrate bias voltage, the CrAlN coating with a higher ratio of Al to Cr showed less chipping and cracks than that with a lower ratio of Al to Cr (Fig. 5a and c, b and d). Figure 5b shows the scratch track of the CrAlN coating with a ratio of Al/(Al + Cr) of 40.0% and a substrate bias voltage of −120 V, less acoustic emission detected during scratching up to 100 N.

Conclusions

CrAlN coatings were deposited on Si and AISI H13 steel substrates by modified ion beam enhanced magnetron sputtering from Cr and Al elemental targets in an Ar + N_2 mixture atmosphere. At the same power of gas ion source, all CrAlN coatings were crystallized in the cubic NaCl B1 structure, showing the (111), (200), and (220) preferential orientation. At the same Al/Cr target power ratio, the (111) diffraction peak decreased in intensity and broadened in width as the bias voltage increased, which is attributed to the variation in the grain size and microstrain. The columnar grain became more compact and dense with increasing substrate bias voltage and Al concentration. At a substrate bias voltage of −120 V and an Al/(Cr + Al) ratio of 40.0%, the coating had the highest hardness and good adhesion to the substrate.

Acknowledgement This work was financially supported by the National Natural Scientific Foundation of China (No. 20471041 and 90306014).

References

1. Heim D, Holler F, Mitterer C (1999) Surf Coat Technol 116–119:530
2. Chiba Y, Omura T, Ichimura H (1993) J Mater Res 8:1109
3. Bin T, Xiaodong Z, Naisai H, Jiawen H (2000) Surf Coat Technol 131:391
4. Mayrhofer PH, Willmann H, Mitterer C (2001) Surf Coat Technol 146–147:222
5. Romero J, Gómez MA, Esteve J, Montalà F, Carreras L, Grifol M, Lousa A (2006) Thin Solid Films 515:113
6. Lin J, Mishra B, Moore JJ, Sproul WD (2006) Surf Coat Technol 201:4329
7. Scheerer H, Hoche H, Broszeit E, Schramm B, Abele E, Berger C (2005) Surf Coat Technol 200:203
8. Brizuela M, Garcia-Luis A, Braceras I, Oñate JI, Sánchez-López JC, Martínez-Martínez D, López-Cartes C, Fernández A (2005) Surf Coat Technol 200:192

9. Brecher C, Spachtholz G, Bobzin K, Lugscheider E, Knotek O, Maes M (2005) Surf Coat Technol 200:1738
10. Spain E, Avelar-Batista JC, Letch M, Housden J, Lerga B (2005) Surf Coat Technol 200:1507
11. Kawate M, Hashimoto AK, Suzuki T (2003) Surf Coat Technol 165:163
12. Ding X-Z, Zeng XT (2005) Surf Coat Technol 200:1372
13. Gannon PE, Tripp CT, Knospe AK, Ramana CV, Deibert M, Smith RJ, Gorokhovsky VI, Shutthanandan V, Gelles D (2004) Surf Coat Technol 189:55
14. Lugscheider E, Bobzin K, Lackner K (2003) Surf Coat Technol 175:681
15. Bobzin K, Lugscheider E, Maes M, Gold PW, Loos J, Kuhn M (2004) Surf Coat Technol 189:649
16. Wuhrer R, Yeung WY (2004) Scr Mater 50(12):1461
17. Uchida M, Nihira N, Mitsuo A, Toyoda K, Kubota K, Aizawa T (2004) Surf Coat Technol 177–178:627
18. Reiter AE, Derflinger VH, Hanselmann B, Bachmann T, Sartory B (2005) Surf Coat Technol 200(7):2114
19. Hirai M, Ueno Y, Suzuki T, Jiang WH, Grigoriu C, Yatsui K (2001) Jpn J Appl Phys 40:1056
20. Moiseev T, Cameron DC (2005) Surf Coat Technol 200:5306
21. Henderson PS, Kelly PJ, Arnell RD, Bäcker H, Bradley JW (2003) Surf Coat Technol 174–175:779
22. Bradley JW, Bäcker H, Kelly PJ, Arnell RD (2001) Surf Coat Technol 142–144:337
23. Bradley JW, Bäcker H, Aranda-Gonzalo Y, Kelly PJ, Amell RD (2002) Plasma Sources Sci Technol 11:165
24. Mišina M, Bradley JW, Bäcker H, Gonzalov YA, Karkari SK, Forder D (2003) Vacuum 68:171
25. Qi D, Rongping L, Shouzhong Z, Jian D (2005) J Vac Sci Technol (China) 25(1):69
26. Endrino JL, Palacín S, Aguirre MH, Gutiérrez A, Schäfers F (2007) Acta Mater 55:2129
27. Karlsson L, Hultman L, Johansson MP, Sundgren J-E, Ljungcrantz H (2000) Surf Coat Technol 126:1
28. Tian L, Zhu X, Tang B, Pan J, He J (2007) Mater Sci Eng A 483–484:751
29. Zhou M, Makino Y, Nose M, Nogi K (1999) Thin Solid Films 339:203
30. Liu ZJ, Shum PW, Li KY, Shen YG (2003) Philos Mag Lett 83:627